

1b. NOVAE DURING OUTBURSTS

OPTICAL STUDIES OF CLASSICAL NOVAE IN OUTBURST

Waltraut C. Seitter

Astronomisches Institut der Westfälischen Wilhelms-Universität
Münster, F.R. Germany

ABSTRACT. A nova is followed optically from preoutburst to postoutburst appearance. Photospheric and atmospheric observational data are explained qualitatively through the energy budget, apparent in super-Eddington, Eddington, and sub-Eddington states, and the particle fluxes, according to their role in Grotrian's model. In some instances, interpretations connected with Grotrian's model are compared to results based on hydrostatic atmosphere models, for which quantitative versions exist. It is hoped that the physically and observationally sound 'Ansatz' of Grotrian may find followers to formulate an updated and extended theory.

Prologue

It is well known that all nova outbursts show a remarkably similar sequence of appearances, which suggests an equally similar sequence of underlying physical processes. Observations covering all wavelength regions from radio radiation to X-rays reveal, during different phases, changes in brightness and energy distribution, and varying strengths, structures, and radial velocities of spectral lines. The data are directly related to energy production, chemistry, and mass ejection of the nova. Additional information is held in the geometry of the outburst. Structures *in projection* become visible in the active phases through line profiles, and during late evolution in the resolved shell; radial velocities together with 2-D images yield 3-D pictures.

The present state of nova research offers physical models to account for a number of observational properties, especially those related to energy generation in the early outburst phases and to nebular physics in the late stages. The energy output is closely associated with the accreted mass and thus with the properties of the binary system, possibly also with the chemical composition of the nova; nebular physics reveals the composition best and traces the chemical evolution of the nova during outburst. Only coarse properties of the intermediate *photospheric* stages have been modelled.

Besides summarizing parts of our knowledge of the various nova stages, the following chapters attempt to account for some of the rich observational detail in a *qualitative* way. It appears that two underlying processes might suffice to model the *behaviour* (not the cause) of the different speed classes, including special features of the light curve and spectral evolution: the varying numbers and masses of the ejected particles and their velocities, as first suggested by Grotrian (1937), *i.e.* the time-dependent *kinetic energy* output, and the time-dependent *luminous energy* output which depends on the rate of energy production and the effectiveness of energy transportation, briefly, on the status of the star as a super-Eddington, Eddington, or sub-Eddington nova. Questions, as to what triggers the observed, sometimes abrupt changes in kinetic energy, in luminous energy, and in the ratio of kinetic to luminous energy are still open.

Definitions

According to the present terminology classical novae are cataclysmic variables (in the modern sense – excluding supernovae) which have shown one and only one major outburst over more than at least 100 years. The following discussion is concerned with the optical properties of the outburst, while the prenova and the postnova stages represent the natural limits for this phase; multiwavelength investigations of novae during outburst are summarized in a recent review (Starrfield 1988).

Using a large collection of observational outburst data for seven novae, McLaughlin (1943) based his classification system on the fact that despite the variety of individual nova properties basic common features can be recognized. His listing of nova stages, exemplified by distinct optical brightness variations and accompanying dominant spectra, remains almost unchanged until today:

The prenova with generally weak brightness variations and the spectrum of a hot star; *the premaximum* with a steep rise towards maximum through the phases *initial rise*, *premaximum halt*, and *final rise*, and a characteristic premaximum spectrum; *the maximum*, including immediate postmaximum and *early decline* with the appearance of the *principal spectrum*, soon followed by the *diffuse enhanced spectrum*; the continued decline and *transition phase* with the *Orion spectrum*, line flaring and coronal lines; the *nebular stage* characterized by forbidden lines; the *postmaximum* with spectra of the stellar and nebular remnant; and *quiescence*.

While optical radiation increases rapidly towards maximum and declines much more slowly to essentially preoutburst magnitude, the spectra develop from absorption line spectra to mixed stages to pure emission line spectra, from permitted to forbidden transitions, from neutral lines and low ionization to high ionization stages, and subsequent return to intermediate ionization. Novae are (almost) uniquely identified on the basis of their light curves, which permit assignment to certain speed classes, and by their maximum spectra. The slight reservation pertains to recurrent novae and a few objects which are difficult to classify, especially since maximum spectra are not available. They will be discussed in Sec. 9. Fast recurrent novae differ spectroscopically from classical novae, and all recurrent novae return to minimum within shorter times than novae. Whether these criteria are necessary and sufficient remains to be seen, as the small group of recurrent novae is enlarged (in the last two years from 5 to 7).

McLaughlin's (1960) excellent review is still worth reading, as is Payne-Gaposchkin's (1957) book, where numerous presentations of light curves, as well as detailed descriptions and illustrations of spectra are given. The fact that many of the model features of 30 years ago differ from those accepted today is more than compensated by the authors' encompassing knowledge of the phenomena, and their sincere attempts to show the physics behind the appearances. Several reviews have been published during the past decennium, and much of the development in the field is summarized in *Classical Novae* by Bode and Evans (1989). The chapter on photoionization models of DQ Her from the Orion phase to the late nebular remnant by Martin (1989) is a rewarding new attempt towards presenting a complete model evolution for a nova. Extensive references to original papers are found in Payne-Gaposchkin (1957) and Duerbeck (1987a).

1 The prenova

1.1 Photometric observations

The single most complete survey of prenova magnitudes is the collection of Robinson (1975), covering 90 years of photographic observations. From the 12 light curves presented by the author, it is apparent that most prenovae for which sufficient data are available show light variations. Furthermore, Robinson concludes, that "usually there is a small increase in luminosity [optical light], 1–15 yr prior to their eruptions". V1500 Cyg which appeared a few weeks after Robinson's paper certainly fits the rule. Years before outburst its blue magnitude was near 21^m , a month before maximum it had reached 16^m and stayed near this magnitude until the onset of the fast rise.

No reliable colour information is available for prenovae. Together with the scarcity of spectra (Sec. 1.2) this makes it impossible to trace the *luminosity* evolution of the prenova and physical changes prior to outburst. The equivalence of the pre- and postoutburst stages within tens of years around the event is, however, not assured as long as the conclusion is based on magnitudes in one spectral region only. No statement is possible on observational grounds concerning time scales of more than a hundred years, with the possible exceptions of CK Vul of 1670 (Shara *et al.* 1985; Sec. 9) and WY Sge of 1783 (Shara *et al.* 1984). On theoretical grounds, the rather small effects of the outburst on the star or system suggest minor differences between prenova and postnova. Statistical and physical considerations, which require more than one outburst per nova, support the assumption of quasi-stability of the underlying star or system.

1.2 Spectroscopic observations

For only three objects prenova spectra are available. All were found on low-resolution objective prism photographs, V603 Aql (1918) on a Henry Draper Catalogue plate, V533 Her (1963) and HR Del (1967) on plates of the Case Institute, the latter also on a Sonneberg plate. The spectrum of V603 Aql does not show the ultraviolet part so that the main characteristic is not visible: the very blue continuum in which at low resolution no lines are detectable. The spectra were taken almost two years (V533 Her), seven years (HR Del) and 19 years (V603 Aql) prior to outburst maximum, and for the two first mentioned novae near the minima in Robinson's prenova light curves.

There is no obvious contradiction to the assumption that the prenova spectrum closely resembles that of the postnova (emission from the ejected shell excluded). Only well-calibrated plates could give reliable continuum distributions, while absorption and emission features would be visible only at much higher resolution. Fig. 1a shows the low-resolution prenova spectrum of HR Del, taken

from Stephenson (1967), considered to be the best prenova spectrum available. For comparison, the spectrum of a neighbouring G5 star is shown in Fig. 1b. At low resolution and with insufficient

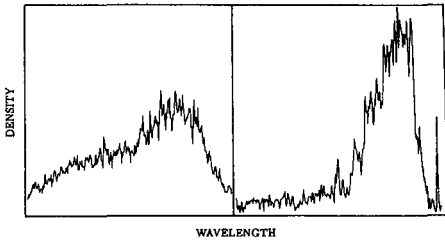


Fig. 1. a) Uncalibrated preoutburst spectrum of HR Del taken by Stephenson on a Ila-O plate 7 years prior to outburst. b) G5-spectrum of neighbouring star on preoutburst plate of HR Del, shown for comparison.

calibration it is not possible to distinguish whether the temperature a few years prior to outburst is of the order 10^4 K, typical for the postmaximum, or of the order 10^5 K, as suggested by a preliminary analysis of the above spectrum. More reliable temperature information on prenovae would help to date the onset of nuclear burning with better confidence than the rise in brightness, which may be masked by variations present throughout the observed premaximum phases.

1.3 Conclusions

Prenova spectra are serendipitous observations on wide-angle objective prism plates, often taken with plate limits not deeper than 10^m to 12^m . This explains why so far only apparently bright novae and/or those with small outburst amplitudes (slow novae) were found at minimum.

At this point I would like to make a plea for a deep objective prism survey reaching at least 18^m and including relatively low galactic latitudes. In spite of the fact that a fairly sizeable collection of sufficiently deep plates has been taken with the UK Schmidt-telescope, a systematic survey is not in sight because of the time-consuming observational work, while considerable progress has been made towards automatic reduction of objective prism plates (Schuecker *et al.* 1989).

1.4 Model Interpretation

- The generally accepted prenova model, selected on the basis of *postnova* properties, is a close binary system with a hot white dwarf surrounded by an accretion disc (except in AM Her-type systems) and a cool, mass transferring companion, usually a main sequence star. Outbursts are due to nuclear runaway reactions on the WD surface. Outbursts can repeat hundreds of times.
- The accretion disc plays a major role in accounting for pre- and postnova brightness and colours of the system, unless the secondary is a cool giant. AM Her-type systems, which, due to the strong magnetic field of the primary, develop only accretion columns may be systematically fainter than systems with accretion discs. This was indeed observed for the AM Her-type nova V1500 Cyg. Hibernation (total loss of the accretion disc) during part of the quiescent stage has been discussed (Shara *et al.* 1986).
- Light variations tens of years before outburst may be due to the companion star and/or processes in the accretion disc. Precursor activity observed during the last few years before outburst may be related to a rise in temperature and loss of the accretion disc, as suggested in the previous paragraph.
- Time scales from postoutburst to preoutburst of 10^4 years were originally estimated from the relation between outburst amplitudes and lengths of outburst cycles given by Kukarkin and Parenago (1934). Today they are estimated on the basis of equality between accreted and ejected mass and range from 10^3 to 10^5 years. Model computations with low accretion rates yield several times 10^5 yr (Priialnik 1989).

2 The premaximum

2.1 Photometric observations

The early steep rise towards light maximum usually lasts for a day or two, the final rise approximately the same time. There are, however, notable exceptions (HR Del). The increase in

magnitude is accompanied by a change towards increasingly redder colours. About 2^m below maximum a phase of constant magnitude, the premaximum halt, may occur (Sec. 3). The final rise is often well observed because the nova is now sufficiently bright to attract attention and to permit studies with good time coverage and high spectral resolution.

2.2 Spectroscopic observations

Premaximum spectra are characterized by a strong blue continuum and blueshifted absorption lines; emission lines are comparatively weak or absent. The line shifts indicate smaller velocities than those observed after maximum. Also, the lines have only one strong component. Invariably, the spectral types deduced from the absorption lines are of earlier type than the maximum and immediate postmaximum spectra (Fig. 2). Three types of line profiles are characteristic for the premaximum spectrum: broad absorption lines, weak P Cygni lines, or P Cygni lines whose emission components decrease before maximum (such as observed in DQ Her and HR Del). In V1500 Cyg, the early premaximum spectrum showed very broad absorption lines. A low-dispersion spectrum of V356 Aql (1936), found on a Vatican astrograph plate taken 10 days before maximum, is not different from a featureless prenova spectrum, though the brightness had already increased by several magnitudes. This suggests that the absorption lines may have been too broad to be visible.

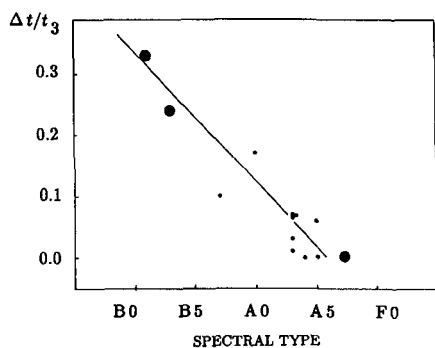


Fig. 2. Changes in spectral types of novae before light maximum ($t = 0$) for time intervals normalized to t_3 -time.

Relative line strengths may deviate from those of normal spectra. The effect was very pronounced in V1500 Cyg, the fastest observed nova with the hottest premaximum spectrum. All major multiplets of C III were unusually strong. Abnormal strengths were also found for He, N, O (Boyarchuk *et al.* 1977), and other elements. The line enhancements may, however, at least partially be due to the extremely low density of the photosphere.

2.3 Conclusions

Evolution of the blueshifted absorption line spectrum towards later types indicates an expanding and cooling photosphere. The presence of only one set of noticeable absorption lines suggests a single major shell. It may have an internal density gradient, in addition to thinning out at both ends due to the velocity dispersion. The broad lines indicate high velocity dispersion.

The *absolute growth of the atmosphere in extent* is determined by the velocities of the ejected gases and by the available time. The *growth in mass* depends on the number of particles traversing the photosphere. Large particle velocities and/or a large particle stream could lead to an extended atmosphere with strong emission lines already in the premaximum stage, unless the evolution towards maximum is fast.

The spectral lines reflect also the *relative growth of atmosphere and photosphere*. An increase in emission line strengths suggests *non-homologous* growth of photosphere and atmosphere, with small positive *photospheric velocities*, i.e. small changes in the growth of the photosphere, due to small increase in particle flux, large increase in particle velocity and/or small changes in opacity. This conditions are best fulfilled during early premaximum rise. *Stable P Cygni lines* suggest *homologous* growth of photosphere and atmosphere and negligible variations in the said properties, conditions which are most likely found during intermediate premaximum rise. *Decreasing emission*

line strengths signal faster growth of the photosphere than of the atmosphere due to large increase in particle flux, small increase in particle velocity and/or rapid increase in opacity. In most novae this appears to be characteristic of the immediate premaximum stage.

The instantaneous position of the photosphere R_p used in the above considerations can be written

$$R_p = f(\text{mass loss, particle velocity}^{-1}, \text{opacity})$$

The original form of this relation was given by Grotrian (1937) and is

$$R_p = R_0 \sqrt{\frac{n_0}{v n_p}}$$

with $R_0 \approx$ prenova radius, n_0 = number of particles ejected through the photosphere per unit surface area and unit time, v = particle velocity, n_p = number of atoms corresponding to a characteristic photospheric density.

A significant *change* in particle velocity within a given shell is not expected. The generally smaller velocities in the premaximum spectrum and the higher ones in the subsequent spectra may be due to different ejection velocities, *i.e.* different acceleration mechanisms and/or strengths in the immediate vicinity of the source.

Changing continuum opacity per unit mass and variable mass loss *strongly affect* the location of the photosphere. The temperature and pressure dependence of the opacity per unit mass is shown in Fig. 3.

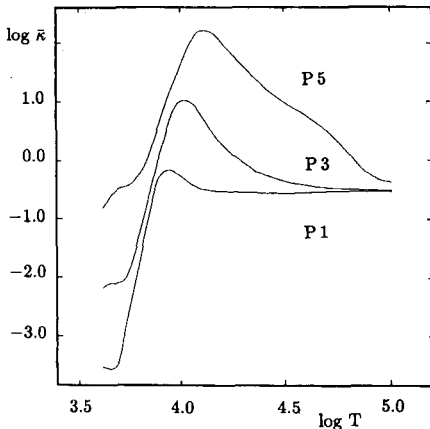


Fig. 3. Changes in mean continuum opacity per unit mass ($\log \bar{\kappa}$) with temperature ($\log T$) for three different pressure values ($\log P$). The data are taken from Vitense (1951). The maxima near 10 000 K correspond to hydrogen recombination, the high temperature slope to bremsstrahlung (free-free absorption), the small hump at low temperatures to the appearance of the H^- -ion, and the flat part to pure Thomson scattering.

During final expansion towards maximum the photospheric temperature declines rapidly, reaching values between 9 000 – 6 000 K for different novae. A simple picture evolves if we can attribute to the nova of a given maximum temperature the pressure which yields maximum opacity at this temperature. For very fast novae, such as V1500 Cyg, with an observed high maximum temperature and the sign of very low density, the photosphere at maximum light may indeed be determined by the maximum opacity per unit mass (Sec. 4.2).

For novae with low maximum temperatures and higher photospheric densities, the opacity may have dropped by as much as two orders of magnitude at maximum light. For constant total mass loss, the optical path length would increase drastically and the photosphere would move inward, contrary to observation. The actually observed rapid growth of the atmosphere can then only be explained by increased mass loss. The fact that the principal absorption spectrum, which appears at maximum, has a higher velocity than the premaximum spectrum suggests that a massive shell has overtaken the premaximum shell and produced the photosphere at maximum.

If at constant luminosity of the central source the particle stream is also constant for a given time interval, the photosphere remains at the same distance from the star and visual brightness stays constant. This happens during the premaximum halt and during a protracted maximum. V1500

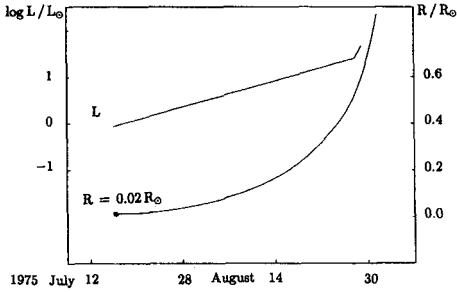


Fig. 4a. Changes in luminosity and radius at constant temperature of V1500 Cyg during early rise to maximum.

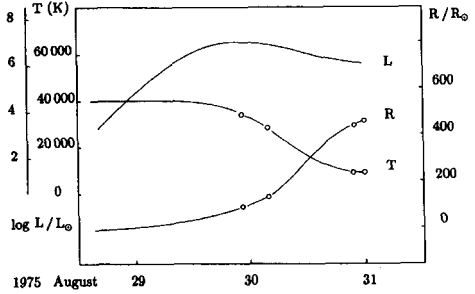


Fig. 4b. Changes in luminosity, radius and temperature of V1500 Cyg during final rise to maximum.

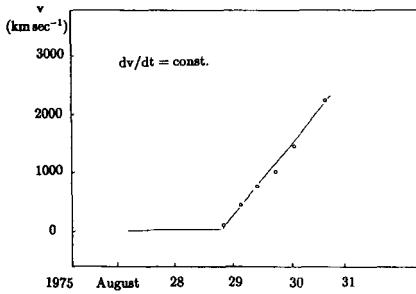


Fig. 5. Increasing photospheric velocity of V1500 Cyg prior to maximum.

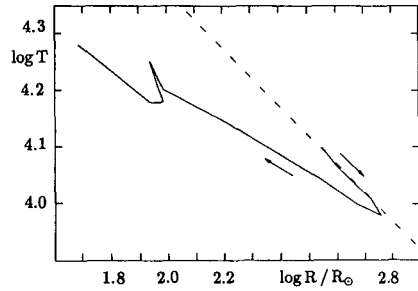


Fig. 6. Evolution near maximum of V1500 Cyg in the temperature/radius diagram. The dotted line represents constant luminosity. V1500 Cyg had a brief constant luminosity phase at maximum luminosity just prior to optical maximum.

Cyg apparently experienced a premaximum *shock ejection* without a subsequent phase of constant mass loss. This may be characteristic for all very fast novae. In Figs. 4a and 4b the evolution of physical parameters in V1500 Cyg is shown. From Fig. 5 it is seen that during final rise the photosphere was driven with *constant acceleration* and that during the final premaximum stages the photosphere grew with almost twice the particle velocity. Fig. 6 shows that V1500 Cyg had no constant luminosity phase *after* maximum. This is in contrast to most novae, where constant maximum luminosity may last for days, weeks or even months after maximum light, as deduced from optical data (Duerbeck and Seitter 1979), and from measurements in the UV and IR (Sec. 4).

2.4 Model interpretation

- A thermonuclear runaway (TNR) in the accreted matter on the surface of the white dwarf ignites noticeably at 10^7 K and, under runaway conditions, reaches the peak burning temperature at or above 10^8 K within seconds to minutes (Starrfield 1989). With CNO burning restricted to the immediate surface layers and sound velocities of the order of the thermal velocities, the outer cooler parts of the accreted layer may experience a shock. The lift-off of a small, over large radii optically thick shell can occur at more than 1000 km s^{-1} above escape velocity.
- Velocity dispersion within the shock gives rise to broad absorption lines.
- The constant acceleration observed during the final rise of V1500 Cyg is determined by five parameters: changing temperature, changing density, changing luminosity, and, because the velocity of the photosphere is so much larger than the particle velocity, nearly constant mass loss. It should thus be possible to derive the behaviour of photospheric pressure near maximum. The simple model of evolution to maximum can be applied to V1500 Cyg and a few other fast novae.

- Unusual line strengths may be due to extreme physical conditions in the expanding shell. Otherwise, they are of chemical origin (Boyarchuk *et al.* 1977). He, N and O could be products of the CNO cycle, C and O could be mixed into the ejecta from the underlying C-O white dwarf. Mixing is also suggested for later phases (Sec. 5).

3 The premaximum halt

3.1 Photometric observations

McLaughlin's typical light curve of novae shows a brief halt in the rise towards maximum light, or even a small decline, at 2^m below optical maximum. Slow novae, however, may experience a protracted halt. In HR Del, the duration of the premaximum halt was exceptionally long and lasted for more than five months. The light curve is shown in Fig. 7. It should be noted that the protracted premaximum phase of HR Del is often considered an extended maximum, an interpretation which fits neither the colour nor the spectroscopic behaviour. Other novae for which a protracted premaximum halt has been suspected are given by Seitter (1969).

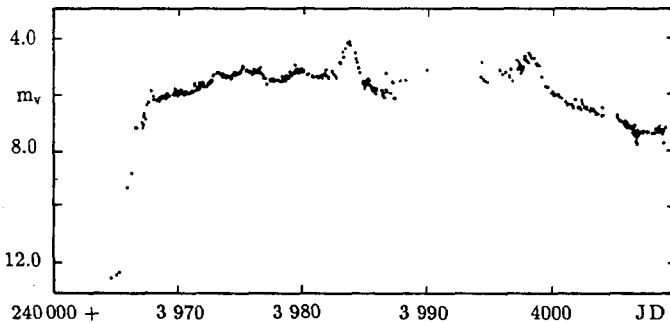


Fig. 7. Light curve of HR Del showing the protracted premaximum halt, the maximum and a secondary maximum. The data are taken from the literature.

3.2 Spectroscopic observations

Because the halt is generally short, about a day or two, little attention is paid to the evolution of spectra during this period. This is different in the case of HR Del. The first brightness plateau of HR Del lasted for about 1.5 months. The spectra taken during this stagnation period show P Cygni profiles typical of a nova near maximum. The sharp blue-shifted absorption lines indicate velocities around 500 km s^{-1} . During the subsequent increase by several $0^m.1$ to a somewhat modulated second plateau, the emission spectrum weakened considerably while the absorption line spectrum became that of a late-type 'super-super' giant. After another 3.5 months, a slow final rise through $1^m.2$ took place, and subsequently HR Del developed the normal principal spectrum of a gradually warming photosphere with emission lines of increasingly higher excitation and ionization energies.

3.3 Conclusions

During the premaximum halt of HR Del, the radius varied by less than 30% (compared to an outburst increase of 8000%), the temperature by less than 10% (compared to at least several 100% during outburst), and the total luminosity by a factor 1.5 (compared to a factor 3000 during outburst). The numbers show that only small variations in mass loss occurred during the prolonged premaximum. The colour evolution is shown in Sec. 4.

3.4 Model interpretation

- In HR Del, the velocity dispersion is small as indicated by the sharp absorption lines. One among several possible causes is that the escape velocity lies in the tail of a peaked (Maxwell-like) distribution of particle velocities and only part of the velocity dispersion becomes observable (see also Sec. 6.4). The majority of particles does not reach escape velocity and falls back into the white dwarf. In novae radiating at the *Eddington limit* this process generates a source for continued mass loss while the large backflow of matter keeps the changes in luminosity small. One thus observes a relatively stable optical brightness. The phase is terminated by a new burst of matter, associated with the principal spectrum.

- Following the long Eddington phase during premaximum, HR Del experienced a weak super-Eddington phase for at least 30 days, starting with a brief optical maximum. Generally, slow novae remain at constant luminosity near the Eddington limit for a prolonged time interval, during which optical brightness declines slowly. In fast, super-Eddington novae the rapid decline in mass loss (no recycling of ejecta) accounts for the rapid decline in optical brightness.

4 Maximum and early decline - principal spectrum

Optical maximum is defined by the peak in the optical light curve, though in rare cases the peak may be a plateau (DO Aql, unless the final rise to maximum was missed and the plateau was an extended premaximum halt). *Spectroscopic maximum* is reached when the principal spectrum becomes dominant. *Physical maximum* is the constant luminosity phase which is transient (V1500 Cyg), lasts for a few to tens of days (usually) or up to 100 days (FH Ser). The photometric maximum does not necessarily coincide with the onset of the spectroscopic maximum (appearance of the principal spectrum).

4.1 Photometric observations

Photometric observations in various colour systems are abundant for the brighter novae near maximum. Colour evolution at this time places the nova in the two-color diagram (UBV system) somewhere between supergiants and black bodies. Nova temperatures can be obtained by interpolating linearly between these two sequences, assuming that the colours are not affected by non-photospheric emission as long as they stay in this regime of the two colour diagram. Colour evolution of four novae is shown in Fig. 8.

4.2 Spectroscopic observations

The principal spectrum is characterized by strong P Cygni lines, generally with multiple components, which may change in strength and number. They are superimposed on a relatively cool and very strong continuum which soon begins to weaken and to become hotter. Absorption lines, which are sensitive to luminosity, may show these effects in a much more pronounced way than even the very bright supergiants (V1500 Cyg). The principal absorption spectrum lasts from maximum through most of the successive stages of nova development until the continuum becomes too weak. Emission lines of hydrogen and metals in low ionization stages (Fe II) are strong and often structured. The early postmaximum spectrum of a slow nova is shown in Fig. 9. Particle velocities deduced from the blueshifts lie in the range of a few to several 100 km s^{-1} for slow novae and of $1000 - 1500 \text{ km s}^{-1}$ for fast novae. Traces of the lower velocity premaximum spectrum are often found during the first few days after maximum.

4.3 Conclusions

The strong radiation maximum observed visually and photographically is due to the temporal coincidence of maximum extent of the photosphere and maximum light emission in the optical part of the spectrum. *Maximum light always occurs at maximum size and minimum photospheric temperature of the nova.* Size and temperature of the photosphere depend on the luminosity of the underlying source and on mass loss; the observed kinetic energy of the ejected particles is determined by the energy set free by the source and the potential well from which the particles escape.

The fairly well established rate of decline/absolute magnitude relation of novae yields absolute magnitudes even if other methods fail. One can thus determine the luminosities and, with known temperatures, also the radii. The instantaneous radii and particle velocities, together with proper values for opacities, yield the ejected masses during given stages. Integrating over all phases of significant mass loss yields the total mass lost during outburst

$$M_{\text{tot}} = \int \dot{M} dt = \int f(R_p, \text{particle velocity, opacity}^{-1}).$$

The changes in photospheric radius and temperature are regulated by mass flow and associated effects on opacity. With declining mass ejection and increasing particle velocities, the photosphere

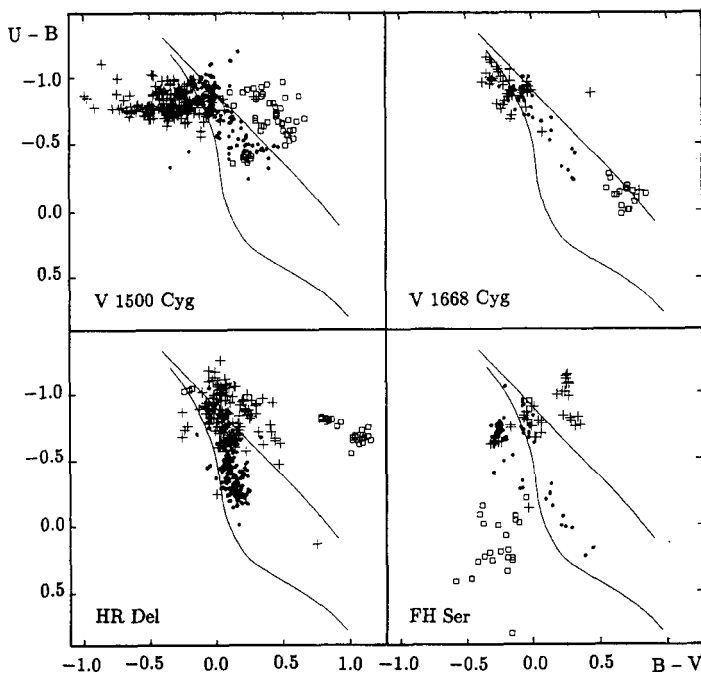


Fig. 8. Two-colour diagrams of four novae, showing 3 characteristic stages of postmaximum evolution. Near maximum and during early decline (dots), the colours are those of a tenuous photosphere and lie between those of the supergiant class Ia sequence (lower curve) and the black body sequence (upper curve). In later decline (crosses), U-B and B-V colours become blue in fast novae, in slow novae B-V turns red. In the transition stage (squares) the B-V colours are generally red, except when circumstellar dust is present, as in the late stages of FH Ser (see text). The data are taken from the literature.

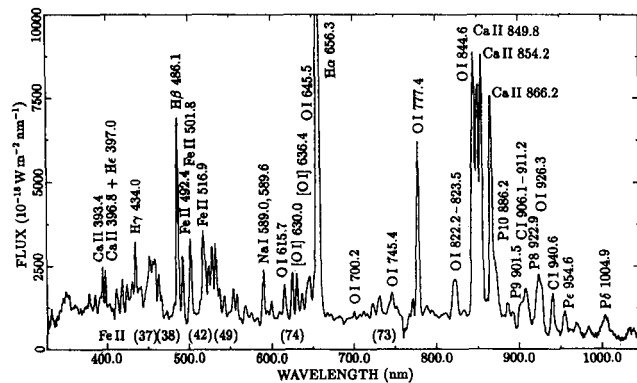


Fig. 9. Early postmaximum spectrum of the slow nova Sct 1989, observed by H.W. Duerbeck and C. Gouiffes on September 25.0, 1989 at the ESO 1.5 m telescope. Fe II multiplet numbers are given in parentheses.

retracts inwards, gets hotter and emits more UV radiation. Optical colour data and the appropriate bolometric corrections show that the luminosity, and thus the luminous energy generating process, in most novae remains constant for some time after light maximum. This is confirmed by observations in the UV, where the radiation maximum of the hot photosphere is located, and, in the presence of dust, by IR measurements of re-radiated light from dust grains, formed in the outer parts of the advancing shell (Sec. 5).

The two-colour diagrams of novae permit further conclusions. Fig. 8 shows that there are generally three phases of colour evolution. Near maximum and during early decline, the nova colours lie between those of bright supergiants and black body colours, of temperatures 6 000 K to 20 000 K.

During the early part of this phase the spectrum is dominated by continuum radiation and the physical parameters mentioned above can be extracted. During the phases of later decline, colours resemble those of hot stars in lower luminosity classes, but in fast novae the increasingly bluer colours in B–V signal large contributions from emission lines in the B-band. The third phase is dominated by red colours in the B–V band, for which the red bremsstrahlung-continuum in the thin atmosphere might be responsible, and/or increasingly stronger [O III]. The colours of deep minima during the transition stage are discussed in Sec. 6.

The evolution during maximum and early postmaximum is characterized by the following processes: The appearance of the strong blueshifted absorption lines of the principal spectrum requires that at least one major shell of high velocity follows the premaximum shell, usually more shells follow. When the principal shell overtakes the premaximum shell, the premaximum lines disappear. The total amount of matter ejected during maximum and postmaximum is much larger than that in the premaximum shell. The *atmospheric phenomena*, increasing strengths of emission lines and first appearance of [O I] lines show the growth of the atmosphere in both mass and extent. The particles producing the diffuse enhanced and the Orion spectrum produce a new continuum against which their absorption lines, together with the strong and long-lasting lines of the principal spectrum are seen.

4.4 Model interpretation

- According to Starrfield (1989), the nova has entered the stage of steady hydrogen burning which could continue for of a few hundred years. The observed short duration of an outburst, however, requires that the process is terminated prematurely. As a possible cause for termination enhanced mass loss due to dynamical friction in the common envelope phase of the outburst has been suggested. The orbiting secondary of the system could impart enough kinetic energy and momentum to give slow moving particles an additional boost (MacDonald *et al.* 1985) so that mass loss is enhanced. The model departs from the Grotrian model.

During the phases when the above process would be most effective, the observed particle velocities are of the order of 1000 km s^{-1} and might still be associated with the ejection itself. Later, when the nova radiates far below the Eddington limit, the star may have reduced to a size smaller than the size of the orbit, so that dynamical friction becomes ineffective. The details of the partition between luminous and kinetic energy in all stages of the nova would have to be known in order to decide whether external processes play a significant role in mass loss. Fully hydrodynamic model calculations (Prialnik 1989) show that very fast novae do not need them because they can start their cooling phases as early as 10 years after outburst.

- Particle velocities are higher in later stages. Well separated absorption components show that matter is ejected in *packets*, i.e. shells or clouds. This can happen when part of the recovered unprocessed material is not immediately re-ejected, but (locally) mixed into the burning region where it initiates brief phases of enhanced energy production and subsequent small shocks. This scheme is in agreement with the observed larger number of shells in near-Eddington novae. At the same time, the packets can account for the irregular light variations, which are also more pronounced in slow near-Eddington novae. A good example is the brief phase of overshooting and subsequent deep drop during the early decline of NQ Vul.
- The empirical maximum light/rate of decline relation describes physically the partition between luminous and kinetic energy. Luminous energy before it reaches the observer is ‘processed’ through the photosphere of the nova. During the outburst of fast and bright super-Eddington novae ‘photospheric processing’ shifts the peak brightness rapidly from the optical to the shorter wavelengths, the more so, the higher the optical brightness at maximum. This, together with the observed high particle velocities, shows that the *ratio of kinetic/luminous energy in the principal ejection is high*.

In Eddington novae ‘photospheric processing’ shifts the radiation maximum more slowly. This is in good agreement with the assumption that backfalling matter, which has not reached the escape velocity, is continually reejected. During the maximum of slow novae, with their low particle velocities, similar visual brightnesses and similar photospheric temperatures, the *ratio kinetic/luminous energy in the principal ejection declines with increasing t_3 -time*.

- In the later phases of decline, when the particle flux is sufficiently reduced, the bremsstrahlung in the growing atmosphere produces the continuum in the long-wavelength part of the spectrum and the colour index B–V becomes larger.

5 Continued decline – diffuse enhanced and Orion spectrum

5.1 Photometric observations

When optical light is reduced by about 1^m.5, the slope of the decline may change and irregular or semiregular light variations of several 0^m.1 are observed in many, except the fastest novae. In most novae the total luminous energy is still the same as at maximum light. Colour measurements begin to be affected by the emission lines and colour indices become less reliable for temperature determinations.

5.2 Spectroscopic observations

The third outburst spectrum, the diffuse enhanced spectrum appears – in very fast novae (V1500 Cyg) one to two days after maximum light, in slow novae one to two weeks. It is characterized by diffuse emission and absorption lines of abundant elements: CNO, Si, S, in some cases Ne, in their first and second ionization stages. The advent of higher ionization lines is characteristic of the Orion spectrum. The line strengths of some elements suggest high abundances.

The velocities of the diffuse enhanced lines are high, those of the Orion spectrum still higher, and the great widths suggest large velocity dispersions; components are often not resolved, and the continuum may have contributions from the merging wings of the emission lines. The principal spectrum is still strong – in absorption, because the continuum or the quasi-continuum from the line wings provide a sufficient background, in emission, because the atmosphere has grown.

5.3 Conclusions

We look into increasingly deeper parts of the expanding shell, into regions of very high temperature, and so do the outer parts of the shell. They receive energetic ionizing and accelerating photons. Here, too, we have to account for shells of different velocities, generally less massive than those ejected during the principal phase.

5.4 Model interpretation

- The energy generating processes are essentially the same as those during the maximum stage, but mass loss has declined to an extent that the continually receding photosphere is much nearer to the energy source and consequently much hotter. Most of the matter accreted onto the nova during quiescence has already been ejected. The material now contains higher percentages of processed material and/or contributions from the white dwarf. In cases where strong Ne lines are observed, the nuclei are mixed-in from an underlying Ne-Mg white dwarf (Williams *et al.* 1985), unless the burning temperature reaches 10⁹ K (Trautvetter *et al.* 1984).
- The high velocities testify of acceleration by high energy photons after the particles have left the photosphere; this is corroborated by the fact that in still later and hotter phases still higher velocities up to the order of several 1000 km s⁻¹ are observed.

6 The transition period – Orion spectrum and flaring

6.1 Photometric observations

Magnitude measurements during the transition period reveal either a smooth decline, quasi-coherent oscillations with typical time scales of 3–15 days, or a deep decline with recovery after some weeks. As early as the 1930s the decline had been attributed to dust forming in the shell and light loss due to absorption, though this hypothesis was not generally accepted. Colour measurements supported the concept of dust absorption. It was finally confirmed by IR astronomy through the detection of re-radiation at long wavelengths while IR spectroscopy revealed the nature of the dust grains. The deep decline may last for a few months.

Optical colour evolution during the deep minimum is illustrated by FH Ser, which developed a thick dust shell (Fig. 8d). At the onset of decline, colours remained approximately the same as

before. Significant changes were observed on the ascending branch, immediately following the faintest V-magnitude (Sec. 6.4).

6.2 Spectroscopic observations

As time proceeds the outer parts of the expanding shell grow so thin and the photosphere is so little restored from the interior, that we see to greater depths than ever before. The broad lines have ionization stages corresponding to the highest ones observed in normal stellar spectra (hot stars in Orion): strong N III 464.0 nm appears in emission, lines of N III and NV in absorption. All lines show structuring.

Light variations during this phase are accompanied by the disappearance and reappearance of lines. Oscillation maxima correspond to the presence of broad Orion lines, oscillation minima to their absence, so that their velocities which start to increase at light maximum cannot be traced to their expected maximum values at light minimum.

An even stronger sign for a thinning atmosphere is the advent of forbidden lines. While auroral and nebular lines of the low ionization stages begin to appear during early decline, prior to and during the transition stage some nova spectra are dominated by coronal and nebular lines. Coronal lines of [Fe X], [Fe XIV], [A XV], [Xe X] are the most common ones in the optical spectrum; a large variety of coronal lines may appear in the IR (Grasdalen and Joyce 1976).

6.3 Conclusions

No phenomenon in the nova evolution is as unexpected as semi-regular light oscillations in a photosphere which owes its existence to rapidly moving particles.

At the oscillation maxima, the particles responsible for the absorption systems have lower velocities. For a given mass loss this leads to larger size. Broad Orion lines suggest high temperature. Large radius and high temperature are in agreement with maximum light. The absence of [O III] lines requires a higher atmospheric density, which suggests high mass loss. Towards the oscillation minima, particles have higher velocities. For a given mass loss this leads to a smaller size of the photosphere. The observed absence of broad Orion lines during the light minima does not imply low temperature, because *narrow* high ionization lines are present. A small radius, in spite of high temperature, is in agreement with minimum light. The presence of [O III] lines requires low density which leads to small mass loss. Consequently, large size of the photosphere, high mass loss, high temperature, and slow particle velocity are correlated at the oscillation maxima. Small size, low mass loss, high temperature, and (extrapolated) high particle velocities are correlated at the oscillation minima. In order for quasi-periodicities to occur in the above correlations, the underlying processes must be self-sustaining over a given time interval.

Coronal lines indicate electron temperatures of a million degrees and electron densities of 10^8 cm^{-3} or lower. They appear just before and during the transition stage at the time of dust formation, which occurs around 1000 K (Gehrz 1988). Coronal lines seem to be emitted in the deep interior of the atmosphere (Grasdalen and Joyce 1976), while dust forms in the outer parts. The required high ionization appears to be due to radiation, rather than shock interaction between the nova and preexisting gas, such as is found in recurrent novae. The late appearance of the coronal lines in novae supports this view.

In lower excitation lines, the existence of numerous components gives evidence of small thin clouds already present or forming during this stage. The cloudlets have much lower temperatures and probably lower densities than the gas found in the major part of the coronal line emitting region; this puts them in the outer regions of the gaseous envelope.

The colour effects of dust absorption are complex and require different particle sizes at different times.

6.4 Model interpretations

- It has been suggested (e.g. Phillips and Selby 1977) that radial pulsations in the nova photospheres are responsible for the observed light variations. The model is derived in the framework of the collapse of a hydrostatic atmosphere (Mustel 1956). In the Grotrian model it does not work because particle velocities near the photosphere, both at maximum and minimum velocity, are so far above escape velocity that it is impossible that they fall back under

the effect of gravity. Light variations in expanding nova envelopes are explained naturally by a modified Grotrian relation and one might attempt to discuss the oscillations within this framework.

Quasi-periodic oscillations appear relatively late in nova evolution, which suggests that the burning layers have dropped into the *sub-Eddington* regime. Mass ejection is reduced and so are particle velocities. Only the fastest ones, in the relatively flat part of an assumed Maxwell-type tail, reach escape velocity. They generate the photosphere at the oscillation minima and account for the comparatively high average velocity, and, due to the missing particles of slower velocities and insignificant contributions from the very distant tail, for the small velocity dispersion. The slower particles fall back, some participate in the burning process and cause a slight retardation in the general decline in luminosity. This is the scene near oscillation minimum (see also Sec. 3.4).

The slightly higher energy thus produced raises the brightness and leads to the ejection of more and faster particles. Assuming that the velocity distribution now peaks nearer to escape velocity, the *average* particle velocity is decreased, because of the large contributions from particles just reaching escape velocity. Due to the flat tail, the high velocities are again less represented than the smaller ones, though they are now more abundant than in the much weaker particle stream near minimum. The velocity dispersion may slowly build up. Also increased is the number of particles which do not reach escape velocity and fall back. They cause further enhancement of burning until the Eddington limit is reached again.

The onset of unstable equilibrium causes a fast depletion of particles. This is the scene near oscillation maximum. With the burning material now reduced, the luminosity falls again below the Eddington limit, the reversed process proceeds until minimum, when a new cycle starts. The process is terminated when the luminosity increase is too small to reach the Eddington limit. Line flaring, in particular nitrogen flaring, which occurs at the oscillation maxima, is due to the increase in the available number of high energy photons (temperature and luminosity increase).

An objection to the above sequence of events may be the apparently sudden onset of the oscillations. There are, however, less regular precursors which mark the gradual approach to the luminosity range below Eddington limit at which the process works best. The incomplete coverage of the light curves during oscillations permits an alternate explanation. The quasi-oscillations could be sequences of small bursts. For this flare-type activity an explanation may require processes in the burning layer, possibly related to deep mixing of back-flowing matter into the white dwarf (see Sec. 4.4).

- The simultaneous presence of an ultra-hot electron gas and of newly formed solid grains can be explained globally in terms of the generally observed ring-blob structure of ejecta (Mustel and Boyarchuk 1970), or locally in terms of small dense clouds shielding their cores from the high energy quanta and providing a nucleation environment. Observations of jet-like gases moving with the velocities of the coronal lines were found in the vicinity of blobs in the nebular remnant of RR Pic (Duerbeck 1987b). If hot gases are ejected only in the direction of the blobs, less shielding is needed in the grain forming ring regions.

Distinct cloudlets, as witnessed by the existence of numerous emission line components, in the resolved nebula as separate condensations, could be the result of Rayleigh-Taylor, Kelvin-Helmholtz or other instabilities in the main stream of ejected matter. They might shield some regions from high energy radiation and keep them cool. It is doubtful, however, that these regions would be dense enough for grain formation considering that the cloudlets themselves have electron densities of less than 10^4 cm^{-3} . If we interpret the light oscillations in the transition stage as due to small energy bursts, they may result in the ejection of numerous thin and quickly dispersing shells of moderately high density. Alternately, a *single* burst may produce a very thin high density shell which decays into instabilities before it becomes large enough to contribute significantly to optical light radiation. The associated small scale height of the layer, which naturally has a negative density gradient, would result in fast-growing dense Rayleigh-Taylor instabilities (Lang 1974), which explain both the fast disappearance of the shell and the formation of small and dense nuclei for dust formation.

- Colour evolution during decline to the deep minimum (at least in the case of FH Ser) can be explained if one assumes that large particles, which have grown rapidly in the outer zones of

the dust forming region, shadow-off the radiation from the stellar source. The rapid growth was possible because in the inner part the dense mini-cloudlets, formed as Rayleigh-Taylor instabilities, shield the outer ones from high energy radiation, at the expense of being able to grow large particles themselves. Particle sizes of $0.6\mu\text{m}$ (Mitchell and Evans 1984) can produce the neutral absorption observed during descent to minimum. Ascent from the deep minimum is the consequence of expansion and thinning of the shell of large particles and the coming into view of the smaller dust grains. They absorb selectively. Alternatively, the larger grains may have been reduced to smaller size by (chemical) sputtering (Mitchell and Evans 1984). On the other hand, dust formation has left a reduced amount of gas in the reappearing atmosphere so that the weaker red contributions from the Grotrian continuum take over and render a blueward shift in B-V while U-B is reddened as determined by the size of the small dust grains.

- Nitrogen which clearly dominates the Orion spectrum is strong in all subsequent phases. A major product of the CNO cycle, it appears in the nova shell after early decline from maximum. Nitrogen may in fact be called the *signature of the nova outburst*. Strong [N II] lines appear throughout the nebular stage. Dominant NV was found in the UV spectra of ejecta from GK Per almost 90 years (Bode *et al.* 1988), in both ring and blobs of RR Pic almost 65 years after outburst. (Duerbeck *et al.* 1989; Seitter *et al.* 1990).

7 Nebular stage

7.1 Photometric observations

The nova has become fainter by several magnitudes. The photosphere is very small and hot and radiates mainly in UV and X-rays (Ögelman *et al.* 1984). A much weaker long-wavelength recombination- and bremsstrahlung-continuum arises high in the atmosphere. Colour measurements are largely determined by emission lines.

7.2 Spectroscopic observations

Forbidden lines characterize the spectrum. In some novae (GQ Mus) coronal lines persist into the nebular stage (Ögelman *et al.* 1984). Auroral lines of O and N, weaken and nebular lines of [O III], [O II], [O I], and [N II] are dominant. Their profiles reflect both global and local structures. Coarse features (e.g. in HR Del) indicate ring-blob geometry, numerous small emission components the presence of as many cloudlets. Fig. 10 shows well-resolved components of [O III] 500.7 nm over a broad base in V842 Cen, Fig. 11 the H β profile in a photographic spectrum of CP Pup (Sanford 1945).

7.3 Conclusions

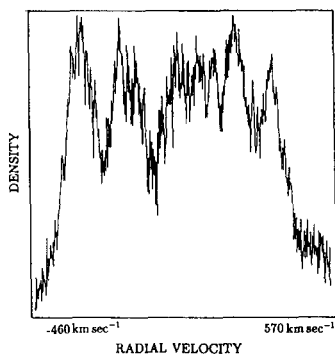
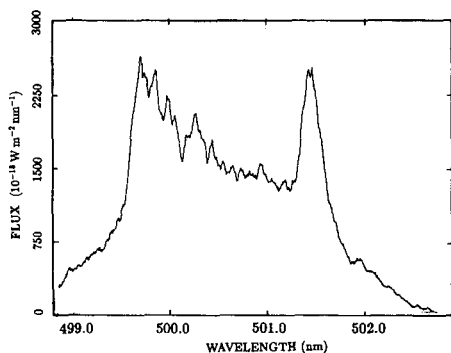
The nebula which has formed around the nova consists of clumpy matter, of numerous cloudlets or blobs. The joint presence of auroral and nebular lines provides the diagnostic tools for temperature and density determinations. The electron temperature is typically around 20 000 K, electron densities per cm^3 are of the order of a few powers of 10. The weakening of auroral lines, the strengthening of nebular lines and the reversal of line ratios sensitive to electron densities trace temperature and density evolution during the nebular stage of the nova.

By that time the formation of cloudlets in the shell is well advanced. High resolution spectra show tens of individual emission lines, each indicating a cloud or bundle of clouds which leave the scene with a given radial velocity component, as seen by the observer. The space velocity is most likely that of the major mass ejection associated with the principal spectrum.

Some of the line components can later be matched with the radial velocities of individually observed blobs. In CP Pup, eleven lines seen during the nebular stage 40 years after outburst could be identified with clouds in the ejecta having the same velocities. The data are given in Table 1.

7.4 Model interpretations

- The atmosphere has developed into an extended shell to which the physics of gaseous nebulae can be applied.



H β components 1943	H α blobs 1981
-454	-457
-354	-229
-236	-229
-133	- 91
- 33	- 69
+ 74	+ 69
+186	+ 91
+262	+ 91
+382	+206
+462	+206
+570	+366

Table 1. Radial velocities in the shell of CP Pup.

Fig. 10. Components of [OIII] 500.7 nm in V842 Cen, observed by H.W. Duerbeck 1988 at ESO 1.4 m CAT with CES.

Fig. 11. Components of H β in CP Pup (November 1943). Adopted from Sanford (1945). Note the entries in Table 1.

- Model computations are used to trace effects of the binary system on the final evolution of the stellar remnant, now sufficiently small to be noticeably affected.

8 The remnant phase

8.1 Observations

The underlying star and the system, before reaching the remnant phase, have undergone major changes: return to their initial states. Photometric and spectroscopic observations indicate that nuclear burning has ceased and that the accretion disk has been regenerated. The gaseous shell has experienced gradual evolution from the nebular to the remnant phase. The appearance of the resolved shell is an important event, it depends, however, much on equipment, observing conditions and reduction methods.

The most striking feature of nova shells, the ring/blob structure, is recognized in a number of cases. The image of FH Ser (Fig. 12) shows structural detail which may be interpreted this way. Observations in the light of different emission lines reveal characteristic patterns in the light of [NII] and [OIII]. In all well-observed nova shells, the former ions concentrate towards the equatorial regions of the shell, the latter towards the polar regions.

8.2 Conclusions

Spatially resolved cloudlets can be used to trace the three-dimensional structure of the shell. Assuming their radial velocities to be projections of the velocity of the component observed in the principal spectrum and taking into account the number of years since outburst, their location in depth is known. The reconstruction of the shell of GK Per (Fig. 13a) leads to the general shape shown in Fig. 13b.

In addition to geometrical information, shell spectroscopy reveals that different parts of the ejecta have noticeable abundance differences. In several remnants a dominance of nitrogen was found in the equatorial ring structure, while the polar blobs show a relative overabundance in oxygen. This

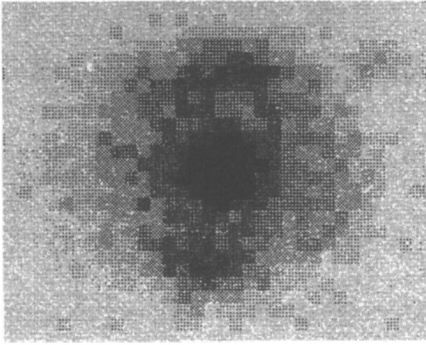


Fig. 12. The shell of FH Ser seen in $H\alpha$ 19 years after outburst, observed by H.W. Duerbeck with the ESO 3.5 m NTT. The diameter is $5''$.

pattern is also present in the apparently irregular shell of GK Per. In Fig. 13a the 'ring' (only visible in images obtained with the colour difference method, not shown here) extends from lower left to upper right and includes the south-west 'bar' (Seitter and Duerbeck 1986).

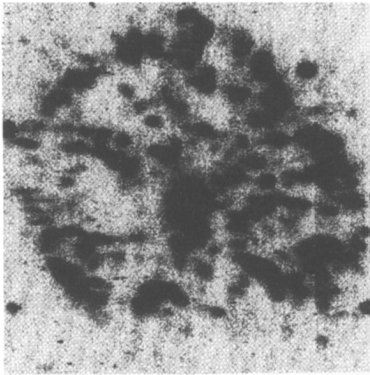


Fig. 13a. The shell of GK Per in the light of $H\alpha + [NII]$ (the latter much stronger) more than 80 years after outburst, observed with the Calar Alto 2.2 m telescope. The diameter is about $80''$.

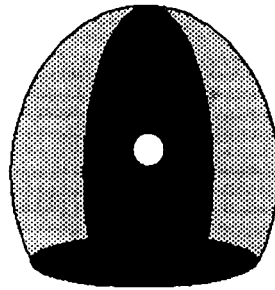


Fig. 13b. Reconstruction of the three-dimensional shell of GK Per using the radial velocities of 200 individual blobs to determine the z -coordinate. Rotated counterclockwise through 45° with respect to Fig. 13a.

8.3 Model interpretation

- The nova model at minimum was introduced in Sec. 1. Return to the fully developed accretion disc depends on the mass loss from the secondary and can typically be completed in some years.
- Particle velocities in the expanding nebula suffer, if any, only small changes. A moderate slowdown is expected from the snow-plow effect – the transfer of kinetic energy and momentum to the swept-up interstellar medium.
- Densities appear to remain constant at $N_e = 10^3 \text{ cm}^{-3}$ for prolonged times, indicating that the cloudlets are in a quasistable state, as expected for Rayleigh-Taylor instabilities. The cloudlets may eventually dissolve and merge into the interstellar medium, probably on time scales not covered by observations. The shells are lost from view much earlier, when the enhancement caused by the superposition of unresolved cloudlets is no longer present because they have drifted too far apart. This may be the case for V603 Aql (Duerbeck 1986).
- Shell ionization does not decline noticeably over the time intervals covered by present observations. The energy supply from the stellar remnant is sufficient in some cases (RR Pic), shocks developing from the interaction between the shell and interstellar or circumstellar gas

provide the energy in others (GK Per). The nature of the energy source is derived from line ratios (Bode *et al.* 1988, Duerbeck *et al.* 1989), using appropriate model calculations.

- Shell structure has been explained in terms of interaction between the ejected shell and the accretion disc. This model requires that the disk still exists at the onset of mass loss. An earlier model is that of Warner (1972) where non-linear pulsations lead to mass ejection in different zones, e.g. in the equatorial belt and the polar caps of the star. Recent observations of magnetic properties in V1500 Cyg at minimum (Kaluzny and Chlebowski 1988, Stockman *et al.* 1988) suggest that the presence of magnetic fields could also play a role.

9 Related objects

V605 Aql and CK Vul are two objects which appear to be novae on the basis of their light curves, but no maximum spectra are available. Both have received much attention during recent times and, if proper novae, would greatly affect current models.

V605 Aql (1919) is discussed by Payne-Gaposchkin (1977) as a peculiar object. It is near the center of an extended faint planetary nebula. A low resolution spectrum taken 2 years after outburst is of C-type. Higher resolution spectra taken at minimum show an unresolved shell which is entirely void of hydrogen. [N II] is present, but the spectrum is dominated by extremely strong lines of [O III], [O II], and [O I], in order of decreasing line strength. Strong C IV 580.6 nm stands out because of its broad line profile. This line, a few marginal broad lines, and a weak highly reddened continuum suggest that the 22^m star is a WR-type planetary nucleus of $T = 10^5$ K which ejected both the planetary and the unresolved nebula (Seitter 1989).

CK Vul was recovered by Shara *et al.* (1985) 300 years after outburst. It is the only known object which could illustrate the late postmaximum stage – if it is indeed a real nova. Because of the extreme importance of the case for nova theory, I shall add to the arguments in favour of this hypothesis, a few possible counterarguments.

The CK Vul complex consists of several clouds with strong H α and [N II] emission, forming a fairly regular ring-blob pattern (Shara *et al.* 1985) around a central object which radiates mostly in the red continuum light. The latter is identified with the central star.

The authors are well aware that the fairly massive ejecta and the very small radial velocities are suggestive of a planetary, though the extreme age of the nova could possibly account for the properties which are different from those normally encountered in a nova. Another problem is the red colour of the central object, unless it is already in hibernation.

Several features would easily fit a V605 Aql-like object. The red colour of the central object, as in the IRAS point source V605 Aql, might be attributed to dust in the system. Another argument against the nova hypothesis are the observed lines of [S II] 671.7, 673.7 nm, which are strong in CK Vul, but *never* observed in nova remnants. Both CK Vul and V605 Aql could be accounted for by the final helium flash in a planetary nucleus. The fact that the observed timescales of outburst are much shorter than predicted by theory is not necessarily an argument against this interpretation, because dynamical models have not yet been computed.

Epilogue

A story of nova outbursts, based on appearances at different times has been told by an optical observer. Some things she has seen with her own eyes, some things she has heard and read, about still others she has speculated (sometimes wildly) – well aware of the fact that solutions are not so simple. The story was not meant to tell what *really* happens during nova outbursts. It is merely a general outline which could be followed in the construction of quantitative models of evolving photospheres of fast moving particles.

Theories concerning the very inside: energy production, evolution of the central star during outburst, element formation, explain a multitude of observations. The late phases of nova evolution are well understood in terms of nebular physics and binary star models. The building of continually changing photospheres in terms of particle ejection, particle velocity and varying absorption coefficients, as suggested by Grotrian, and questions relating to energy partition between luminous and kinetic energy, have not received the same detailed attention. The incomplete story told here is the call of the observer to the theoretician.

Acknowledgements

Sincere thanks go to A. Bruch, R. Duemmler, H.W. Duerbeck, H.-A. Ott and H.-J. Tucholke for valuable discussions and for critically reading the manuscript, to R. Duemmler also for obtaining the scans of old nova spectra, to R. Budell for photographic work, and to B. Cunow and M. Tacke for extensive graphical and editorial help.

References

- Bode, M.F., Duerbeck, H.W., Seitter, W.C., Albinson, J.S., Evans, A., 1988. In *A Decade of UV Astronomy with IUE*, ESA SP-263, p. 665.
- Bode, M.F., Evans, A., 1989. *Classical Novae*, J. Wiley, Chichester.
- Boyarchuk, A.A., Galkina, T.S., Krasnobabtev, V.I., Rachkovskaya, T.M., Shakhovskaya, N.I., 1977. *Sov. Astr.*, **21**, 257.
- Duerbeck, H.W., 1986. *Mitt. Astr. Ges.*, **65**, 207.
- Duerbeck, H.W., 1987a. *A Reference Catalogue and Atlas of Galactic Novae*, D. Reidel, Dordrecht = *Space Sci. Rev.*, **45**, 1.
- Duerbeck, H.W., 1987b. *ESO Messenger*, No. 50, 8.
- Duerbeck, H.W., Seitter, W.C., 1979. *Astr. Astrophys.*, **75**, 297.
- Duerbeck, H.W., Seitter, W.C., Bode, M.F., Evans, A., 1989. These proceedings.
- Gehrz, R.D., 1988. *Ann. Rev. Astr. Astrophys.*, **26**, 377.
- Grasdalen, G.L., Joyce, R.R., 1976. *Nature*, **259**, 187.
- Grotian, W., 1937. *Z. Astrophys.*, **13**, 215.
- Kaluzny, J., Chlebowski, T., 1988. *Astrophys. J.*, **332**, 287.
- Kukarkin, B.V., Parenago, P.P., 1934. *Perem. Zv.*, **4**, 51.
- Lang, K.R., 1974. *Astrophysical Formulae*, Springer, Heidelberg, p. 318.
- MacDonald, J., Fujimoto, M.Y., Truran, J.W., 1985. *Astrophys. J.*, **294**, 263.
- Martin, P.G., 1989. In *Classical Novae*, eds. Bode, M.F., Evans, A., J. Wiley, Chichester, p. 73, 93, 113.
- McLaughlin, D.B., 1943. *Publ. Michigan Obs.*, **8**, 149.
- McLaughlin, D.B., 1960. In *Stellar Atmospheres*, (*Stars and Stellar Systems* Vol. VI), ed. Greenstein, J.L., University of Chicago Press, Chicago, p. 585.
- Mitchell, R.M., Evans, A., 1984. *Mon. Not. R. Astr. Soc.*, **209**, 945.
- Mustel, E.R., 1956. in *Vistas in Astronomy*, ed. Beer, A., Pergamon Press, London, p. 1486.
- Mustel, E.R., Boyarchuk, A.A., 1970. *Astrophys. Space Sci.*, **6**, 183.
- Ögelman, H., Beuermann, K., Krautter, J., 1984. *Astrophys. J.*, **287**, L31.
- Payne-Gaposchkin, C., 1957. *The Galactic Novae*, North-Holland, Amsterdam.
- Payne-Gaposchkin, C., 1977. In *Novae and Related Stars*, ed. Friedjung, M., D. Reidel, Dordrecht, p. 3.
- Phillips, J.P., Selby, M.J., 1977. *Astrophys. Space Sci.*, **49**, 339.
- Prialnik, D., 1989. These proceedings.
- Robinson, E.L., 1975. *Astr. J.* **80**, 515.
- Sanford, R.F., 1945. *Astrophys. J.* **102**, 357.
- Schuecker, P., Horstmann, H., Seitter, W.C., Ott, H.-A., Duemmler, R., Tucholke, H.-J., Tacke, M., Teuber, D., Meijer, J., Cunow, B., 1989. *Reviews of Modern Astronomy*, **2**, ed. Klare, G., Springer, Heidelberg (in press).
- Seitter, W.C., 1969. In *Non-periodic Phenomena in Variable Stars*, ed. Detre, L., Academic Press, Budapest, p. 277.
- Seitter, W.C., 1989. In *Planetary Nebulae*, ed. Torres-Peimbert, S., Kluwer, Dordrecht, p. 315.
- Seitter, W.C., Duerbeck, H.W., 1986. In *RS Ophiuchi and the Recurrent Nova Phenomenon*, ed. Bode, M.F., VNU Science Press, Utrecht, p. 71.
- Seitter, W.C., Duerbeck, H.W., Evans, A., Bode, M.F., 1990. To be published.
- Shara, M.M., Moffat, A.F.J., McGraw, T.J., Dearborn, D.S., Bond, H.E., Kemper, E., Lamontagne, R., 1984. *Astrophys. J.*, **292**, 763.
- Shara, M.M., Moffat, A.F.J., Webbink, R.F., 1985. *Astrophys. J.*, **294**, 271.
- Shara, M.M., Livio, M., Moffat, A.F.J., Orio, M., 1986. *Astrophys. J.*, **311**, 163.
- Starrfield, S., 1988. In *Multiwavelength Astrophysics*, ed. Cordova, F., Cambridge University Press, Cambridge, p. 159.
- Starrfield, S., 1989. In *Classical Novae*, eds. Bode, M.F., Evans, A., J. Wiley, Chichester, p. 39
- Stephenson, C.B., 1967. *Publ. Astr. Soc. Pacific*, **79**, 584.
- Stockman, H.S., Schmidt, G.D., Lamb, D.Q., 1988. *Astrophys. J.*, **332**, 282.
- Trautvetter, H.P., Görres, J., Kettner, K.U., Rolfs, C., 1984. In *Stellar Nucleosynthesis*, eds. Chiosi, C., Renzini, A., **109**, D. Reidel, Dordrecht, p.79.
- Vitense, E., 1951. *Z. Astrophys.*, **28**, 81.
- Warner, B., 1972. *Mon. Not. R. astr. Soc.*, **160**, 35p.
- Williams, R.W., Ney, E.P., Sparks, W.M., Starrfield, S.G., Wyckoff, S., Truran, J.W., 1985. *Mon. Not. R. Astr. Soc.*, **212**, 753.